Ann. For. Res. 67(1): 155-166, 2024
https://doi.org/10.15287/afr.2024.3457

ANNALS OF FOREST RESEARCH
www.afrjournal.org

Vegetation predicts soil shear strength in Arctic soils: Ground-based and remote sensing techniques

Wade A. Wall[1], Ryan Busby[1]✉, Lauren Bosche[2]

Wall W.A., Busby R. Bosche L., 2024. Vegetation predicts soil shear strength in Arctic soils: Ground-based and remote sensing techniques. Ann. For. Res. 67(1): 155-166.

Abstract Soil shear strength (SSS) is an important soil attribute that is influenced by vegetation. If aboveground biomass estimates can be used to predict soil shear strength, it would greatly enhance our ability to estimate SSS across large areas. Using data collected from 24 plots in Alaska, we analyzed the relationship between soil shear strength and ground-collected vegetation attributes and remotely sensed (RS) variables. We constructed both univariate and multivariate models to assess the predictive capabilities of the vegetation and RS variables. Total trees and total conifers were significant predictors of SSS, with a negative relationship existing between total trees/total conifers and SSS. Graminoid cover (%) was positively correlated with soil shear strength and was also a significant predictor of SSS. Of the RS variables, the bands B1 (0.443 µm), B2 (0.490 µm), and B3 (0.560 µm) from the Sentinel 2 satellite system were all significant predictors of SSS. A multivariate model improved model fit over the simple univariate models, with an $R^2 = 0.46$. We have both demonstrated a connection between SSS and aboveground vegetation attributes for areas within interior Alaska and that it is possible to link SSS to RS variables using a multivariate model.

Keywords: soil shear strength, remote sensing, Alaska, boreal forest.

Addresses: [1]US Army Corps of Engineers, Engineer Research and Development Center, Construction Engineering Research Laboratory, Champaign, IL, USA| [2]US Army Corps of Engineers, Engineer Research and Development Center, Cold Regions Research and Engineering Laboratory, Fort Wainwright, AK, USA.

✉ **Corresponding Author:** Ryan Busby (ryan.r.busby@usace.army.mil).

Manuscript: received January, 12, 2024; revised June 26, 2024; accepted June 30, 2024.

Introduction

Vegetation-soil relationships have global implications and affect numerous ecosystem processes. For example, soil spatial heterogeneity has long been recognized as a key driver of plant species distributions (Figueiredo et al. 2018). Soil physical and chemical properties influence not only distribution patterns but plant speciation as well (Anacker et al. 2011). In turn, vegetation can affect ecosystem processes. Nutrient cycling (Hobbie 1992), hydrology (Arora 2002), and carbon storage (Gu et al. 2019) are all known to be affected by vegetation. Understanding the complex interactions

between vegetation and soil, especially under changing global climate patterns, is critical for increasing our understanding of ecosystems in flux and to better predict the effects of these vegetation-soil interactions. In addition, increased understanding of vegetation-soil relationships should lead to better predictive models and a better understanding of the impact of anthropogenic activities (e.g. logging (Pohjankukka et al. 2016), agriculture (Raper 2005), recreational activities (Sutherland et al. 2001)) on the environment.

Soil shear strength, defined as the shear stress a soil can withstand before failure, is an important soil property affecting multiple environmental processes. For example, erosion processes are influenced by soil shear strength (Watson & Laflen 1986), even on low slopes (Léonard & Richard 2004). Soil shear strength is also a major determinant of soil failure, especially during large rainfall events (Yalcin 2007), which can ultimately lead to catastrophic landslides. Soil shear strength's impacts on environmental processes can, in turn, influence, and be influenced by anthropogenic activities. Both intrinsic and extrinsic factors can influence soil shear strength.

Mineralogy of a given soil greatly impacts soil shear strength (Wu 1996), with quartz and feldspar (large particles) and halloysite, kaolinite, mica, and smectite (clay minerals) being positively correlated with slope stability (Tiwari & Marui 2005). Particle size distribution is also known to have an influence on soil shear strength (Wang et al. 2013). In general, smaller particle sizes lead to increased soil shear strength through particle cohesion. Another intrinsic factor affecting soil shear strength is the angularity of the soil particles (Suh et al. 2017), with well-rounded particles having reduced soil shear strength relative to particles with sharper angles. The main extrinsic factors influencing soil shear strength are soil moisture (Gerard 1965), compaction, and vegetation (Operstein & Frydman 2000).

Vegetation increases soil shear strength through increasing the cohesion strength of soils (De Baets et al. 2008). Soils without roots have a lower cohesion force relative to soils with roots (Hu & Zhu 2009), with vegetation increasing slope stabilization and thus preventing erosion (Löbmann et al. 2020), even for slopes with reduced vegetation due to fire or grazing (De Baets et al. 2006). This becomes especially important in saturated soils, as saturated soils, especially on slopes, are more prone to failure. Failure can result in increased erosion, formation of gullies, and in extreme cases, possibly catastrophic landslides (Hoffman et al. 2018).

Multiple studies have investigated predicting soil strength from vegetation (root) characteristics. For example, slope stabilization has been shown to be positively impacted by forest age and composition, with older stands of mixed composition demonstrating increased soil strength (Schmidt et al. 2001). In some areas, grasslands have been shown to have a reduced capacity to resist slippage relative to slopes with shrubs (Terwilliger & Waldron 1991). Related to slope stabilization, the effects of vegetation on erosion control have been investigated and several factors have been identified. Deeper root systems are more effective for controlling erosion relative to more shallow root systems (Brown et al. 2010). Results such as these have been used to incorporate root characteristics into soil strength models (Waldron 1977, Waldron & Dakessian 1981), essentially by adding the combined contribution of roots to soil strength.

Models that attempt to encapsulate the contribution of roots to soil strength contain varying levels of complexity. Early, simpler models only required the tensile strength of root fibers per unit area (Wu et al., 1979), but several studies found that the model overestimated the root contribution (Preti & Giadrossich 2009), leading to increasingly complex models that require measurements or estimates of root area, diameter, cross sectional area, number of roots, root length, etc. (Ji et al. 2020). Most of these experiments have been performed in the laboratory. Field tests

have identified the variability of lab-produced results and generally corroborate laboratory-based models (Shoop et al. 2015).

Unfortunately, for most of these studies, it is unclear how to increase the spatial extent of the results without extensive field data collection. For example, even using the simplest soil strength model presented by Wu et al. (1979) would require estimating root tensile strength, which likely varies widely across vegetation communities with differing species composition. While physics-based models can extend our mechanical understanding of soil strength and the relationships between above- and below-ground vegetation with soil strength, a bridge between soil strength and observable dependent variables is required to extend the applicability of soil strength knowledge.

In the current study, our objectives are to identify if aboveground vegetation measurements and satellite imagery can effectively be utilized to predict soil shear strength variation in boreal forests. Across two summers (2021-2022), we measured soil shear strength using a shear vane across 24 plots in Alaska and compared the results to both ground-based vegetation measurements and remotely sensed (RS) satellite imagery. We performed a series of univariate and multivariate spatial regression analyses on assembled variables and report the results. Finally, we interpret the results in relation to processed-based soil shear strength models that include vegetation and identify paths forward for model improvement.

Materials and Methods

Site characteristics

Forested areas were selected across interior Alaska to represent a diversity of boreal forest types (Fig. 1). Forest types were classified as either hardwood, mixed, black spruce, white spruce, and mixed spruce dependent on the dominance of tree species in each plot. We did not use the forest classifications in any formal analyses; plots were simply classified to obtain a diversity of boreal forest types. In total, 24 plots were measured at five sites (Farmer's Loop, Creamer's Field, Horseshoe Lake, Johnson Road, and Donnelly Training Area), comprised of seven hardwood, five mixed, two black spruce, six white spruce, and four mixed spruce plots.

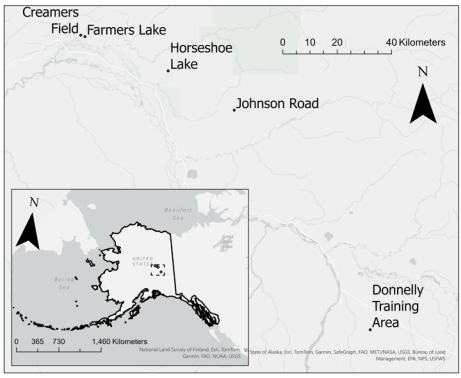

Figure 1 Map of five sampling sites in interior Alaska (inset).

Field and remote sensing data collection

At each plot, a center point was marked and GPS coordinate were obtained. From each center point, a circle with a 14.6 m diameter was created by marking 7.3 m from the center point in each cardinal direction, following United States Forest Service Forest Inventory and Analysis (FIA) Guidelines (USFS 2020). In each quadrant of the circle, 35 random shear vane samples were collected to a depth of 10 cm using an H-227 Field Shear Vane (Humboldt Manufacturing, Elgin, IL, USA) using a 25.4 x 50.8 mm tip.

In 2021, vegetation data collection followed USFS (2020) guidelines and included measurement of diameter at breast height (DBH) and height and identification of all trees with DBH > 12.45 cm, a microplot with 2.07 m radius was established and all saplings were identified with DBH and height measured. All vascular plant species occurring at > 1% cover were identified and assigned a FIA cover classification. All non-vascular plants within subplots were grouped as either feathermoss or

Spaghnum. A habitat type was assigned to each subplot to Level IV of the Alaska Vegetation Classification (Viereck et al. 1992).

Forest density, slope, and aspect were recorded and additional data describing disturbance, permafrost, and soil properties were collected. As most of these variables exhibited no relationship with soil shear strength after the first year of data collection, the sampling protocol was simplified so that only those variables exhibiting relationships were retained for the 2022 data collection efforts to increase sampling efficiency. In 2022, the number of trees greater than 10 cm DBH were recorded by species in each plot. A 0.25 m^2 quadrat was used to measure grass, graminoid, and moss percent cover to the nearest 5% with five random locations per circle quadrant. Depth to mineral soil was measured at a single point in each quadrant and frost depth was measured using a frost probe in five random locations per quadrant.

Sentinel 2A satellite imagery (Drusch et al. 2012) was downloaded for each of the 24 plots using Google Earth Engine (Gorelick et al. 2017). Sentinel 2A is part of the Copernicus program that collects imagery, for most bands, at the 10-meter scale roughly every 5 days. We selected cloud-free images based on proximity to the field data collection date. For each of the downloaded satellite images, we calculated the normalized Difference Vegetation Index (NDVI) using the formula *NIR-Red/NIR+Red* where *NIR* is the near infrared band and *Red* is the red band. In addition, we calculated the tasseled cap indices brightness, greenness, and wetness for each image (Kauth & Thomas 1976). The tasseled cap indices are generated by multiplying the individual satellite bands by sensor-specific coefficients. For the Sentinel 2A images, we used the coefficients generated by Shi and Xu (2019). The resulting image thus consisted of the original Sentinel 2A bands, as well as the additional bands NDVI, greenness, wetness, and brightness (Table 1). For each of the 24 plots, we calculated the mean value for each of the satellite variables, as plot size overlapped multiple pixels.

Table 1 RS variables included in data analysis and their abbreviations.

Predictor	Abbreviation
Coastal Aerosol (0.443 nm)	B1
Blue (0.490 nm)	B2
Green (0.560 nm)	B3
Red (0.665 nm)	B4
Vegetation red edge (0.705 nm)	B5
Vegetation red edge (0.740 nm)	B6
Vegetation red edge (0.783 nm)	B7
Near infrared (0.842 nm)	B8
Narrow near infrared (0.865 nm)	B8A
Shortwave infrared (1.610 nm)	B11
Shortwave infrared (2.190 nm)	B12
Normalized Difference Vegetation Index	NDVI
Brightness	Brightness
Greenness	Greenness
Wetness	Wetness

Data analysis

For summary statistics, we generated histograms for each dependent variable to assess the dependent variable distribution. To assess the relationships between ground-collected and RS variable, we generated a correlation matrix (Pearson 1900) for all the dependent variables (Table 1). For all the ground-collected and RS variables, we fit a simple non-spatial univariate linear regression model regressed on the shear vane values. As standard, we set the significance level (α) at 0.05; p-values less than 0.05 indicated significant differences between models with independent variables and without (null models). Next, we tested for spatial correlation among plots using Moran's I (Gittleman & Kot 1990) for each dependent variable. Moran's I measures spatial autocorrelation and provides a metric from which a p-value can be generated. P-values < 0.05 indicate significant spatial autocorrelation. The null hypothesis is that there is no spatial correlation; test statistics with p-values < 0.05 are considered evidence of spatial correlation.

For predictor variables that did not exhibit spatial correlation (i.e. p-values for Moran's I were > 0.05), we used the non-spatial simple

linear regression previously referenced and tested against a null model that did not include the dependent variable using the ANOVA function in R (R Development Core Team, 2021) package car (Fox 2019). If Moran's I detected evidence of spatial correlation, we used a spatial regression model that accounts for spatial autocorrelation as implemented in the R package spaMM (Rousset & Ferdy 2014). We included the spatial coordinates in a Matérn covariance function (Stein 1999). We used a likelihood ratio test to compare the spatial model fit against a null model that only included the spatial coordinates as random effects using the LRT function in the R package spaMM.

For the ground-collected dependent variables that were significant, we constructed bivariate models that included two of the dependent variables (e.g. total trees and graminoid cover) in addition to an interaction term. Despite our low sample sizes, we decided to include the analyses for exploratory purposes. We tested for inclusion of an interaction term and a second variable using the ANOVA function in the base package within R. Finally, we included five of the RS variables into a final model for predicting soil strength. RS variables were selected based on whether the variable was (a) identified as significant in a univariate model and (b) not highly (> 0.8) correlated with another included RS variables, or (c) a calculated index (e.g. NDVI) that was subjectively identified as likely being important to include in a predictive model. We used a ridge regression model (Hoerl & Kennard 1970) available in the R package Glmnet (Friedman et al. 2010) to reduce overfitting, as many of the RS variables suffered from multicollinearity. We first scaled the variables, centered on 0 with a standard deviation of 1, and selected the best lambda using cross validation.

Results

Most of the field collected and remotely sensed (RS) variables exhibited a relatively uniform distribution of values. The only exception to this was average hardwood DBH: the values were either 0 or large, with very few measurements in the middle sizes (data not shown). While the non-spatial regression model indicated a significant fit, the results are spurious, and we removed the variable from further consideration.

Many of the ground-collected and RS variables were significantly correlated (Table A1). For the ground-collected variables, there were several expected correlations. The highest identified correlation was 0.6 for total trees and total conifers. Average conifer DBH was 0.59. There was a negative correlation between total trees and graminoid cover (-0.67). There was a negative correlation between total conifers and several of the RS variables. Many of the RS variables were highly correlated, with most of the Sentinel 2A bands and the calculated indices mostly having positive correlation values > 0.5. The outlier was the tasselled cap derived index wetness, which was negatively correlated with all the RS bands except for the Sentinel 2A bands B1 (coastal aerosol) and B2 (blue).

Several ground-based vegetation variables were correlated with soil strength (Figure 2). Since every ground-based vegetation variable exhibited spatial autocorrelation based on Moran's I, we only used the regression model that accounted for spatial correlation. The total number of trees was negatively correlated with shear vane values (Table 2), as was the total number of conifers in a plot. Conversely, graminoid cover was positively correlated with shear vane values, meaning that soil strength increased as graminoid cover increased. As expected, total trees and total conifers variables were negatively correlated with graminoid cover (Table A1). However, when total trees, graminoid cover, and their interaction were included in a simple linear regression model, a comparison of nested models indicated that neither interaction term was necessary (P = 0.31) nor graminoid cover (P = 0.15).

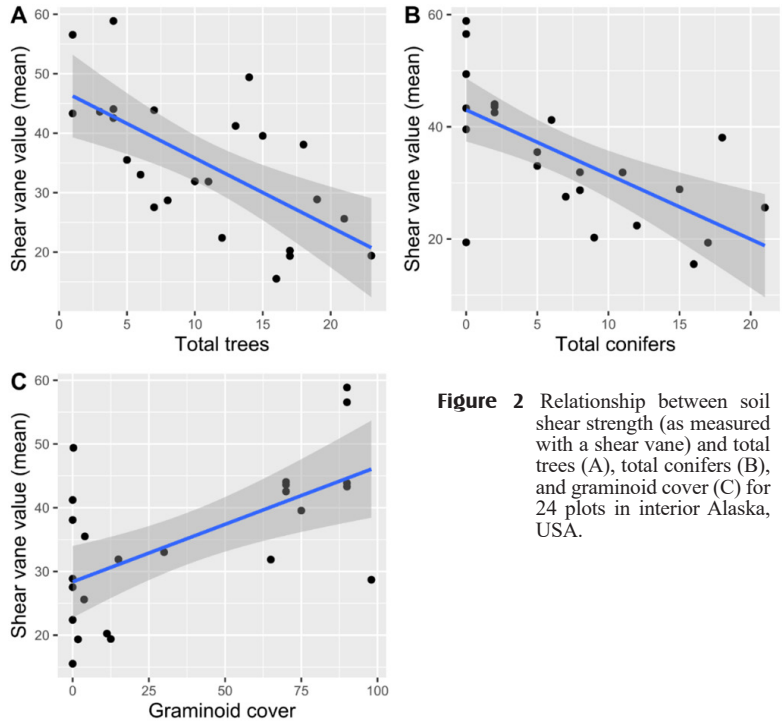

Figure 2 Relationship between soil shear strength (as measured with a shear vane) and total trees (A), total conifers (B), and graminoid cover (C) for 24 plots in interior Alaska, USA.

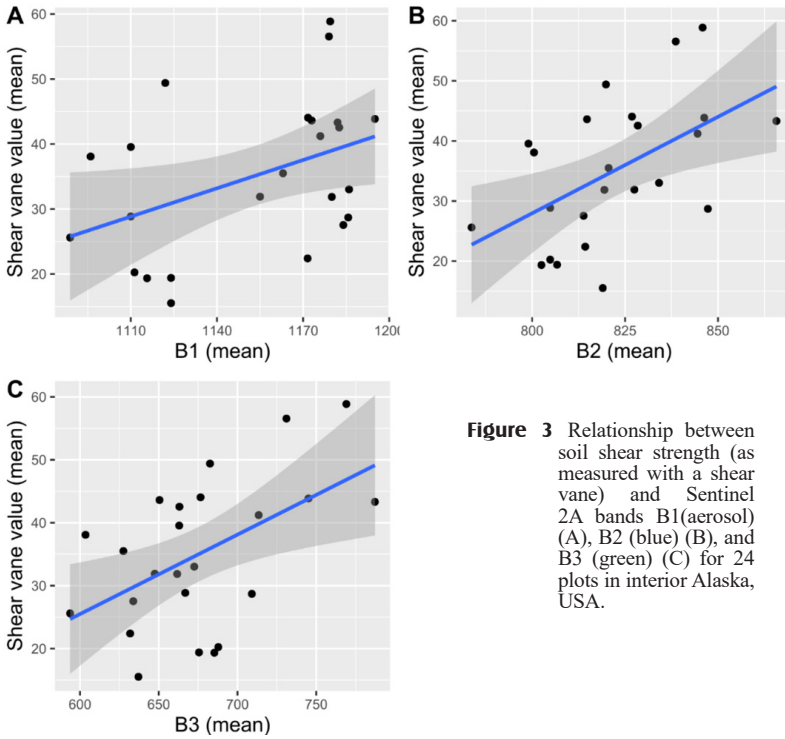

Figure 3 Relationship between soil shear strength (as measured with a shear vane) and Sentinel 2A bands B1(aerosol) (A), B2 (blue) (B), and B3 (green) (C) for 24 plots in interior Alaska, USA.

A univariate model with only total trees was sufficient and had an adjusted R^2 of 0.40 (versus an adjusted R^2 of 0.43 for the full model with an interaction term and an adjusted R^2 of 0.43 for the bivariate model with total trees and graminoid cover).

Table 2 Simple linear (simple) or spatial regression (spatial) intercept, slope, and significance values for 23 ground-based and remotely sensed variables regressed on shear vane soil strength estimates.

Variable	Model	Intercept	Slope	Sign.
Total trees	spatial	49.206	-1.265	<0.001
DBH (mean)	simple	<0.001	0.468	0.696
Total conifers	spatial	42.67	-1.277	<0.001
Conifer DBH (mean)	spatial	38.028	-0.906	0.103
Total hardwoods	spatial	33.918	0.008	0.985
Hardwood DBH (mean)	simple	28.203	1.489	0.019
Graminoid cover	spatial	28.268	0.179	0.002
Moss cover	simple	39.899	-0.120	0.053
B1 (mean)	spatial	-170.937	0.178	0.016
B2 (mean)	spatial	-221.032	0.311	0.007
B3 (mean)	spatial	-170.937	0.178	0.016
B4 (mean)	spatial	-21.746	0.146	0.082
B5 (mean)	spatial	7.181	0.041	0.100
B6 (mean)	spatial	11.927	0.010	0.244
B7 (mean)	spatial	14.328	0.008	0.310
B8 (mean)	spatial	28.296	0.003	0.434
B8A (mean)	spatial	24.175	0.004	0.509
B11 (mean)	spatial	27.443	0.006	0.370
B12 (mean)	spatial	27.351	0.015	0.387
Brightness	spatial	10.231	0.005	0.276
Greenness	spatial	31.062	0.002	0.501
Wetness	spatial	33.171	-0.003	0.591
NDVI	spatial	-13.664	65.763	0.279

Note: Sing.: significance

As with the ground-based vegetation variables, RS variables exhibited significant spatial autocorrelation. Inclusion of several RS bands improved soil strength estimate model fit (Table 2). Sentinel 2A bands B1 (coastal aerosol; 443 nm), B2 (blue; 490 nm), and B3 (green; 560 nm) specifically were positively correlated with soil strength (Figure 3). These three RS variables were positively correlated, with B1 and B2 having a Pearson correlation value of 0.8 and B2 and B3 having a correlation value of 0.79. Inclusion of B1 significantly increased model fit (X_1^2 = 5.8; P = 0.016), as did B2 (X_1^2 = 7.17; P = 0.007), and B3 (X_1^2 = 6.4; P = 0.011). All other RS variables, including the calculated indices, did not significantly improve soil shear strength model fit.

The final ridge regression model included the Sentinel 2A bands B1 and B3, as well as the calculated bands wetness and NDVI. Model results indicated an adjusted R^2 of 0.46 (Figure 4).

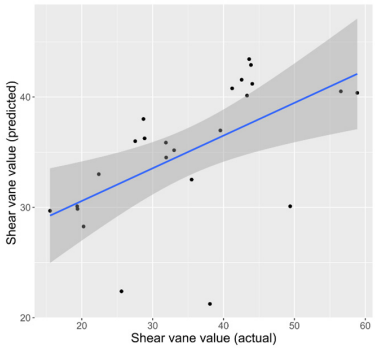

Figure 4 Shear vane measured (actual) and predicted values based on a ridge regression model that included the remote sensing variables B1, B3, wetness, and NDVI for 24 plots in interior Alaska.

Discussion

Soil shear strength was correlated with several aboveground ground-collected vegetation and RS variables across 24 plots in interior Alaska (Figure 1). Inclusion of total trees (count), total conifers (count), and graminoid cover (%) improved model fit when trying to predict soil strength (Table 2), with soil strength negatively correlated with total trees/conifers and positively correlated with graminoid cover (Figure 2). The relationship between aboveground vegetation properties and soil strength has been observed across different areas of the world. Examples include plant cover (specifically graminoid) being correlated with scree stabilization in the Italian Alps (Giupponi et al. 2023), vegetation cover (and root density) correlated with vegetation and species richness in Korea (Ali et al. 2017), and plant species diversity correlated with soil

stability in experimental plots in Germany (Pérès et al. 2013). However, most studies have focused on connecting belowground biomass (specifically root mass/density) with soil strength. This is understandable, as belowground biomass is the direct driver for increasing soil strength, with aboveground vegetation attributes (e.g., cover, functional diversity) being correlated with belowground biomass and not necessarily the direct driver of soil strength. The focus on the connections between belowground biomass and soil strength hamper the ability to extend inferences spatially, as belowground biomass estimates are more difficult to obtain relative to aboveground biomass.

Fortunately, there are known relationships between aboveground and belowground biomass (Naesset 2004, Cheng & Niklas 2007, Smyth et al. 2013) that point to the potential ability to use aboveground vegetation measurements as a surrogate for belowground biomass. Previous studies (Enquist & Niklas, 2002, Niklas 2004) have shown aboveground biomass scales with belowground biomass across a wide range of plant sizes. However, there is some uncertainty as to whether the observed relationships continue to hold true in mixed forest stands and across forest types, with some authors finding some support for relationships across mixed forests (Zianis & Mencuccini 2004), while other authors questions the existence of "universal" scaling factors (Li et al. 2005). If the allometric relationships do span diverse taxonomic groups of plants and forest types, then it leads to a greater potential to use aboveground measurements, either ground-based or RS, for estimating soil strength. This increases the ability to extend the spatial extent of predictive models, as belowground biomass measurements are not as easily scalable as aboveground. However, a recent global study indicated that the belowground percentages of plant biomass differ by vegetation type (Ma et al. 2021).

A further extension is linking aboveground vegetation and RS variables. This is a necessary step for increasing the spatial extent of soil strength modeling, as ground-based vegetation measurements, while more cost effective than below-ground vegetation measurements, are still costly in terms of time and financial resources (Ali et al. 2016). In the current study, univariate spatial regression models that included Sentinel 2A bands B1, B2, and B3 improved soil strength estimates, relatively to null models that did not include these variables (Table 2). All three bands were positively correlated with soil strength, and negatively correlated with total trees and total conifers (Table A1). The negative correlation between B1 and total trees was quite high (-0.85). None of the Sentinel 2A bands were correlated very strongly with graminoid cover, through B3 had the highest positive correlation (0.64). Interestingly, none of the derived bands (brightness, greenness, wetness, NDVI) were highly correlated with the vegetation variables. We had initially expected that derived bands may perform better for both identifying total trees or grasslands, as derived bands have previously been used successfully to assess grasslands (Ali et al., 2016). The crosswalk from ground-based to RS variables requires the development of training sets. In our current study, the identified correlations between the vegetation and RS variables, and the ability of RS variables to be utilized to predict soil strength, allowed for the establishment of this linkage. We provide these connections for boreal forests and associated grasslands, but at the present time the applicability of the identified relationships between vegetation and RS variables to different biomes or outside our area of study is unclear.

While the use of univariate RS variables provided improved model fit relative to null models, the combination of multiple RS variables (specifically bands B1, B3, wetness, and NDVI) increased the ability of RS variables to predict soil strength (Figure 4).

The inclusion of the calculated bands NDVI and wetness, which when used in a univariate model did not significantly increase model fit (Table 2), increased the R2 by ~ 0.20 (data not shown). The multivariate model results should be treated as exploratory in nature, as the sample size of the data (24) is likely not robust enough. To conclude, the model results should be viewed as a path forward for additional study and expansion into additional biomes and ecosystems. Further, as soil properties were not investigated, including analysis of soil properties known to influence soil strength, such as mineralogy (Wu, 1996), particle size distribution (Wang et al., 2013), soil moisture (Gerard, 1965), etc. will only improve the accuracy of predictions. In 2021, all of our study sites were in areas where mineral soil was far below the level where shear strength sampling was conducted. In 2022, depth to mineral soil was much more variable and shear vane measurements at some sites were primarily conducted in mineral soils. However, as soil analyses were not conducted, these variables were not included in the analyses but inclusion of even basic soil data will likely improve the model considerably.

There are both spatial and temporal limitations to our univariate and multivariate model results. As referenced above, different vegetation communities and biomes will have different remote sensing signatures (da Silva et al. 2022). Thus, it is likely that separate models would need to be constructed for different community types across geographical regions. At the present time, based on our limited sampling (Figure 1), it is unclear as to the spatial extent with which inferences can be drawn, both geographically and by community type. For example, would models constructed in riparian areas in Alaska be transferrable to the continental United States? It is also likely that our results are temporally constrained. Previous work looking at the transferability of soil strength models through time (years) indicated a loss of predictive power from one image to the next (Sopher et al. 2016). This area deserves more attention but requires multi-year studies with data collected at the same point through multiple time steps.

Even with these caveats, our results have demonstrated that both ground-based vegetation data and RS bands can be used to construct predictive models of soil strength. While our results have spatial and temporal limitations, they do provide a roadmap for paths toward robust models of soil strength. To do this, it will be necessary to collect multi-temporal data points across a wide range of vegetation community types and include additional environmental variables. The most efficient methodological approach would be to identify broad vegetation community types (likely by biome), collect multi-temporal vegetation and soil data, and compare these data to similar biomes across different geographical areas. This would allow identifying which biomes (or other large vegetation community classes) may be adequate for modeling purposes and which ones are not, as well as the important underlying soil properties that should be included.

Conclusions

In this paper, we have demonstrated that remote sensing bands from the Sentinel 2 satellite system can be utilized to predict soil shear strength in artic soils. While we acknowledge that our sample size is relatively small, the present study presents a path forward toward a more cost-effective means of estimating soil shear strength that can be spatially extended to additional physiographic regions.

Compliance with ethical standards

Conflict of interest

The authors declare no conflict of interest.

Acknowledgments

The authors would like to thank Jeff Mason and Bryan Strong (Salcha-Delta Soil and Water Conservation District) for plot establishment

and data collection, Steph Saari (US Army Cold Regions Research and Engineering Laboratory) for data collection assistance, Dan Rees (Fort Wainwright) for providing FIA plot establishment and sampling guidance, and Tom Douglas (US Army Cold Regions Research and Engineering Laboratory) for site selection assistance. This research was funded by the US Department of Defense - PE 0602182A and 633463AR4, Applied Research Project 'Extreme Cold Weather Threats and Dependencies'.

Supporting information

Table S1 Correlation matrix for ground-based and remotely sensed variables for 24 vegetation plots in interior Alaska.

References

Ali H.E., Reineking B., Münkemüller T., 2017. Effects of plant functional traits on soil stability: Intraspecific variability matters. Plant and Soil 411: 359–375. https://doi.org/10.1007/s11104-016-3036-5

Ali I., Cawkwell F., Dwyer E., Barrett B., Green S., 2016. Satellite remote sensing of grasslands: from observation to management. JPECOL 9: 649–671. https://doi.org/10.1093/jpe/rtw005

Anacker B.L., Whittall J.B., Goldberg E.E., Harrison S.P., 2011. Origins and consequences of serpentine endemism in the California flora. Evolution 65: 365–376. https://doi.org/10.1111/j.1558-5646.2010.01114.x

Arora V., 2002. Modeling vegetation as a dynamic component in soil-vegetation-atmosphere transfer schemes and hydrological models. Reviews of Geophysics 40(2): 3-1-3-26. https://doi.org/10.1029/2001RG000103

Brown R.N., Percivalle C., Narkiewicz S., DeCuollo S., 2010. Relative rooting depths of native grasses and amenity grasses with potential for use on roadsides in New England. HortScience 45: 393–400. https://doi.org/10.21273/HORTSCI.45.3.393

Cheng D.-L., Niklas K.J., 2007. Above- and below-ground biomass relationships across 1534 forested communities. Annals of Botany 99: 95–102. https://doi.org/10.1093/aob/mcl206

da Silva A.R., Demarchi L., Sikorska D., Sikorski P., Archiciński P., Jóźwiak J., Chormański J., 2022. Multi-source remote sensing recognition of plant communities at the reach scale of the Vistula River, Poland. Ecological Indicators 142: 109160. https://doi.org/10.1016/j.ecolind.2022.109160

De Baets S., Poesen J., Gyssels G., Knapen A., 2006. Effects of grass roots on the erodibility of topsoils during concentrated flow. Geomorphology 76: 54–67. https://doi.org/10.1016/j.geomorph.2005.10.002

De Baets, S., Poesen J., Reubens B., Wemans K., De Baerdemaeker J., Muys B., 2008. Root tensile strength and root distribution of typical Mediterranean plant species and their contribution to soil shear strength. Plant and Soil 305: 207–226. https://doi.org/10.1007/s11104-008-9553-0

Drusch M., Del Bello U., Carlier S., Colin O., Fernandez V., Gascon F., Hoersch B., Isola C., Laberinti P., Martimort P., 2012. Sentinel-2: ESA's optical high-resolution mission for GMES operational services. Remote Sensing of Environment 120: 25–36. https://doi.org/10.1016/j.rse.2011.11.026

Enquist B.J., Niklas K.J., 2002. Global allocation rules for patterns of biomass partitioning in seed plants. Science 295(5559): 1517–1520. https://doi.org/10.1126/science.106636

Figueiredo F.O.G., Zuquim G., Tuomisto H., Moulatlet G.M., Balslev H., Costa F.R.C., 2018. Beyond climate control on species range: The importance of soil data to predict distribution of Amazonian plant species. Journal of Biogeography 45(1): 190–200. https://doi.org/10.1111/jbi.13104

Fox J., Weisberg S., 2019. An R companion to applied regression, 3rd ed. Sage Publications. [Google Scholar].

Friedman J., Hastie T., Tibshirani R., 2010. Regularization paths for generalized linear models via coordinate descent. Journal of Statistical Software 33(1): 1-22. https://doi.org/10.18637/jss.v033.i01

Gerard C.J., 1965. The influence of soil moisture, soil texture, drying conditions, and exchangeable cations on soil strength. Soil Science Society of America Journal 29, 641–645. https://doi.org/10.2136/sssaj1965.03615995002900060017x

Gittleman J.L., Kot M., 1990. Adaptation: statistics and a null model for estimating phylogenetic effects. Systematic Zoology 39(3): 227–241. https://doi.org/10.2307/2992183

Giupponi L., Leoni V., Pedrali D., Zuccolo M., Cislaghi A., 2023. Plant cover is related to vegetation and soil features in limestone screes colonization: A case study in the Italian Alps. Plant and Soil 483: 495–513. https://doi.org/10.1007/s11104-022-05760-3

Gorelick N., Hancher M., Dixon M., Ilyushchenko S., Thau D., Moore R., 2017. Google Earth Engine: Planetary-scale geospatial analysis for everyone. Remote Sensing of Environment 202: 18–27. https://doi.org/10.1016/j.rse.2017.06.031

Gray D.H., Barker D., 2004. Root-soil mechanics and interactions. Riparian Vegetation and Fluvial Geomorphology 8: 113–123. https://doi.org/10.1029/008WSA09

Gu X., Fang X., Xiang W., Zeng Y., Zhang S., Lei P., Peng C., Kuzyakov Y., 2019. Vegetation restoration stimulates soil carbon sequestration and stabilization in a subtropical area of southern China. Catena 181: 104098. https://doi.org/10.1016/j.catena.2019.104098

Hobbie S.E., 1992. Effects of plant species on nutrient

cycling. Trends in Ecology & Evolution 7: 336–339. https://doi.org/10.1016/0169-5347(92)90126-V

Hoerl A.E., Kennard R.W., 1970. Ridge regression: Biased estimation for nonorthogonal problems. Technometrics 12(1), 80–86. https://doi.org/10.2307/1271436

Hoffman C.M., Sieg C.H., Linn R.R., Mell W., Parsons R.A., Ziegler J.P., Hiers J.K., 2018. Advancing the science of wildland fire dynamics using process-based models. Fire 1(2): 32. https://doi.org/10.3390/fire1020032

Hu L., Zhu J., 2009. Determination of the tridimensional shape of canopy gaps using two hemispherical photographs. Agricultural and Forest Meteorology 149(5): 862–872. https://doi.org/10.1016/j.agrformet.2008.11.008

Ji J., Mao Z., Qu W., Zhang Z. 2020. Energy-based fibre bundle model algorithms to predict soil reinforcement by roots. Plant and Soil 446: 307-329. https://doi.org/10.1007/s11104-019-04327-z

Kauth R.J., Thomas G.S., 1976. The tasselled cap–a graphic description of the spectral-temporal development of agricultural crops as seen by Landsat. In: LARS Symposia. p. 159.

Léonard J., Richard G., 2004. Estimation of runoff critical shear stress for soil erosion from soil shear strength. Catena 57: 233–249. https://doi.org/10.1016/j.catena.2003.11.007

Li H.-T., Han X.-G., Wu J.-G., 2005. Lack of evidence for 3/4 scaling of metabolism in terrestrial plants. Journal of Integrative Plant Biology 47(10): 1173–1183. https://doi.org/10.1111/j.1744-7909.2005.00167.x

Löbmann M.T., Geitner C., Wellstein C., Zerbe S., 2020. The influence of herbaceous vegetation on slope stability – A review. Earth-Science Reviews 209: 103328. https://doi.org/10.1016/j.earscirev.2020.103328

Ma H., Mo L., Crowther T.W., Maynard D.S., van den Hoogen J., Stocker B.D., Terrer C., Zohner C.M., 2021. The global distribution and environmental drivers of aboveground versus belowground plant biomass. Nat Ecol Evol 5: 1110–1122. https://doi.org/10.1038/s41559-021-01485-1

Niklas K.J., 2004. Plant allometry: is there a grand unifying theory? Biological Reviews 79(4): 871–889. https://doi.org/10.1017/S1464793104006499

Operstein V., Frydman S., 2000. The influence of vegetation on soil strength. Proceedings of the Institution of Civil Engineers - Ground Improvement 4: 81–89. https://doi.org/10.1680/grim.2000.4.2.81

Pearson K., 1900. On the criterion that a given system of deviations from the probable in the case of a correlated system of variables is such that it can be reasonably supposed to have arisen from random sampling. The London, Edinburgh, and Dublin Philosophical Magazine and Journal of Science 50: 157–175.

Pérès G., Cluzeau D., Menasseri S., Soussana J.-F., Bessler H., Engels C., Habekost M., Gleixner G., Weigelt A., Weisser W.W., 2013. Mechanisms linking plant community properties to soil aggregate stability in an experimental grassland plant diversity gradient. Plant and Soil 373: 285–299. https://doi.org/10.1007/s11104-013-1791-0

Pohjankukka J., Riihimäki H., Nevalainen P., Pahikkala T., Ala-Ilomäki J., Hyvönen E., Varjo J., Heikkonen J., 2016. Predictability of boreal forest soil bearing capacity by machine learning. Journal of Terramechanics 68: 1–8. https://doi.org/10.1016/j.jterra.2016.09.001

Preti F., Giadrossich F., 2009. Root reinforcement and slope bioengineering stabilization by Spanish Broom (*Spartium junceum* L.). Hydrology and Earth System Sciences 13: 1713–1726. https://doi.org/10.5194/hess-13-1713-2009

R Development Core Team, 2021. R: a Language and environment for statistical computing.

Raper R.L., 2005. Agricultural traffic impacts on soil. Journal of Terramechanics 42: 259–280. https://doi.org/10.1016/j.jterra.2004.10.010

Rousset F., Ferdy J.-B., 2014. Testing environmental and genetic effects in the presence of spatial autocorrelation. Ecography 37, 781–790. https://doi.org/10.1111/ecog.00566

Schmidt K., Roering J., Stock J., Dietrich W., Montgomery D., Schaub T., 2001. The variability of root cohesion as an influence on shallow landslide susceptibility in the Oregon Coast Range. Canadian Geotechnical Journal 38(5): 995–1024. https://doi.org/10.1139/t01-031

Shi T., Xu H., 2019. Derivation of tasseled cap transformation coefficients for Sentinel-2 MSI at-sensor reflectance data. IEEE Journal of Selected Topics in Applied Earth Observations and Remote Sensing 12: 4038–4048. https://doi.org/10.1109/JSTARS.2019.2938388

Shoop S.A., Coutermarsh B., Cary T., Howard H., 2015. Quantifying vegetation biomass impacts on vehicle mobility. Journal of Terramechanics 61: 63–76. https://doi.org/10.1016/j.jterra.2015.05.001

Sopher A.M., Shoop S.A., Stanley J.M., Tracy B.T., 2016. Image Analysis and Classification Based on Soil Strength (Final Report No. 16–13). ERDC-CRREL, Hanover, NH.

Stein M.L., 1999. Interpolation of spatial data: some theory for kriging. Springer Science & Business Media.

Suh H.S., Kim K.Y., Lee J., Yun T.S., 2017. Quantification of bulk form and angularity of particle with correlation of shear strength and packing density in sands. Engineering Geology 220: 256–265. https://doi.org/10.1016/j.enggeo.2017.02.015

Sutherland R.A., Bussen J.O., Plondke D.L., Evans B.M., Ziegler A.D., 2001. Hydrophysical degradation associated with hiking-trail use: a case study of Hawai'iloa Ridge Trail, O'ahu, Hawai'i. Land Degradation & Development 12(10): 71–86. https://doi.org/10.1002/ldr.425

Terwilliger V.J., Waldron L.J., 1991. Effects of root reinforcement on soil-slip patterns in the Transverse Ranges of southern California. Geological Society of America Bulletin 103(6): 775–785. https://doi.

org/10.1130/0016-7606(1991)103<0775:EORROS>2.3.CO;2

Tiwari B., Marui H., 2005. A new method for the correlation of residual shear strength of the soil with mineralogical composition. Journal of Geotechnical and Geoenvironmental Engineering 131(9): 1139–1150. https://doi.org/10.1061/(ASCE)1090-0241(2005)131:9(1139)

USFS, 2020. United States Forest Service Forest Inventory and Analysis Guidelines.

Viereck L.A., Dryness C., Batten A., Wenzlick K., 1992. The Alaska Vegetation Classification (No. PNW-GTR-286). US Department of Agriculture, Forest Service, Pacific Northwest Research Station, Portland, OR.

Waldron L.J., 1977. The shear resistance of root-permeated homogeneous and stratified soil. Soil Science Society of America Journal 41, 843–849.

Waldron L.J., Dakessian S., 1981. Soil reinforcement by roots: calculation of increased soil shear resistance from root properties. Soil Science 132, 427–435.

Wang J.-J., Zhang H.-P., Tang S.-C., Liang Y., 2013. Effects of particle size distribution on shear strength of accumulation soil. Journal of Geotechnical and Geoenvironmental Engineering 139(11): 1994–1997. https://doi.org/10.1061/(ASCE)GT.1943-5606.00009

Watson D.A., Laflen J.M., 1986. Soil strength, slope, and rainfall intensity effects on interrill erosion. Transactions of the ASAE 29(1): 98–102. https://doi.org/10.13031/2013.30109

Wu T., 1996. Soil strength properties and their measurements. Landslides - Investigation and Mitigation. Special Rep. No. 247. Washington, DC.

Wu T.H., McKinnell III W.P., Swanston, D.N., 1979. Strength of tree roots and landslides on Prince of Wales Island, Alaska. Canadian Geotechnical Journal 16, 19–33.

Yalcin A., 2007. The effects of clay on landslides: A case study. Applied Clay Science 38: 77–85. https://doi.org/10.1139/t79-003

Zianis D., Mencuccini M., 2004. On simplifying allometric analyses of forest biomass. Forest ecology and management 187(2-3): 311–332. https://doi.org/10.1016/j.foreco.2003.07.007